Materials Physics and Mechanics 42 (2019) 423-435 Received: May 24, 2019

INVESTIGATION AND MODELING THE AUSTENITIZATION KINETICS OF STEELS WITH COMPLEX MICROSTRUCTURE UNDER CONTINUOUS HEATING

A.A. Vasilyev*, D.F. Sokolov, S.F. Sokolov, A.I. Rudskoy

Peter the Great St. Petersburg Polytechnic University, Polytekhnicheskaya, 29, 195251, St. Petersburg, Russia

*e-mail: vasilyev_aa@mail.ru

Abstract. An experimental investigation of the austenitization under continuous heating of various microstructures of 8 industrial steel grades with wide range of chemical compositions was carried out. A quantitative mathematical model describing the austenitization kinetics of the steels with complex microstructure and predicting austenite grain size in dependence on the chemical composition, volume fractions of structural components (ferrite, pearlite, bainite, martensite), ferrite grain size and heating rate, was developed. Values of the model empirical parameters were defined basing on the obtained data on kinetics of austenitization, as well as on the measured final austenite grain size. All experiments were performed using the Pocket Jaw unit of the Gleeble 3800 complex. The kinetics of austenitization and the austenite grain size predicted by the developed model are in good agreement with experimental data.
Keywords: steels, austenitization kinetics, continuous heating, mathematical modeling

1. Introduction

Many heat treatment processes of steels include heating, when their partial or complete austenitization occurs. The resulting structure, in particular the austenite grain size, significantly affects the final structure of steel formed during the subsequent cooling, and its mechanical properties. Consequently, a number of papers [1-19] are devoted to the experimental studies of this process, as well as to the development of corresponding mathematical models. Compared with austenite transformation under cooling, when its development is mainly determined by the chemical composition of steel and the austenite grain size, the austenitization kinetics and the resulting grain size depend on much more factors. Along with the chemical composition, these factors include the size and spatial distribution of cementite particles, volume fractions and morphology of the components of initial structure, as well as the heating rate of steel from room temperature to a holding temperature [2,4,5,7-9,11-13,17]. Interest in austenitic transformation has increased significantly due to the development of technologies for production of dual-phase steels, their final structure being formed during rapid cooling after exposure in the intercritical temperature range [3,6,10,13,18,19].

Up to now, a significant number of mathematical models have been developed to describe the austenitization kinetics [5,11,15,18,19], some of them are considered in the review [16]. It should be noted that most of these models relate to austenitization of steels of a certain chemical composition with initial ferritic-pearlitic structure [5,11,15,16,18,19]. This moment makes it impossible to use them for modeling this process in steels with other chemical compositions and initial structure.

http://dx.doi.org/10.18720/MPM.4242019_7
© 2019, Peter the Great St. Petersburg Polytechnic University
© 2019, Institute of Problems of Mechanical Engineering RAS

This paper presents results of experimental investigation of the austenitization under continuous heating of various microstructures of 8 industrial steel grades with wide range of chemical compositions, as well as a quantitative mathematical model for describing the austenitization kinetics and predicting the final austenite grain size, taking into account the effects of chemical composition.

2. Investigated steels, experimental procedures and results used in model calibration

Investigated steels and experimental procedures. Austenitization kinetics under continuous heating was studied for 8 industrial steel grades with chemical compositions presented in Table 1. The investigated samples were made from plates of these steels hot rolled on the mill 2800 of PJSC "Severstal".

Table 1. Chemical compositions of the investigated steels (mass.%)

Steel	C	Mn	Si	Cr	Ni	Cu	Mo	Nb	V	Ti
45Х *	0.45	0.68	0.31	0.96	0.06	0.12	0.01	0.003	0.004	0.003
65Г *	0.66	0.95	0.33	0.10	0.09	0.11	0.01	0.002	0.002	0.002
12Х1МФ *	0.13	0.56	0.20	0.94	0.21	0.13	0.26	0.002	0.152	0.002
13ХФА *	0.12	0.44	0.23	0.61	0.07	0.12	0.02	0.024	0.054	0.003
АБ2 *	0.08	0.37	0.25	0.41	1.94	0.52	0.25	0.002	0.031	0.003
18ХГНМФР *	0.20	1.47	0.30	0.85	1.49	0.28	0.28	0.041	0.124	0.063
14ХГ2САФД *	0.17	1.55	0.56	0.64	0.26	0.14	0.03	0.002	0.051	0.002
S690	0.12	0.97	0.30	1.08	0.24	0.17	0.52	0.033	0.006	0.003

* Russian steel grades.

Before studying the austenitization under continuous heating from room temperature at rates of 0.5, 1, 3, 10, 50°C/s steel samples were thermally pre-treated in the following regime: heating (5°C/s) up to 1000°C → exposure 60 s → cooling (50°C/s) to 900°C → cooling at selected rates to room temperature. At the final cooling two cooling rates were used, providing for formation of microstructures of various desired types, which were the initial structures when studying the austenitization. These cooling rates were selected on the basis of performed study of the austenite decomposition during continuous cooling of steels under consideration and the resulting microstructures.

To obtain special microstructures for identifying the boundaries of former austenite grains formed during austenitization and for measuring their size, a series of additional experiments were carried out. In these experiments immediately after reaching 1000°C at continuous heating the samples were cooled according to regimes that ensure formation of either microstructures with a grid of ferrite formed along the austenite grain boundaries or mixed microstructures of lath bainite and martensite. Such microstructures made it possible to "draw" up a continuous grid that runs along the boundaries of former austenite grains and to determine their average size. Samples for metallographic study were cut at the thermocouple location. The ATM system was used for the preparation of analytical sections. The austenite grain size was determined by means of Carl Zeiss Axio Observer microscope supplied with the Thixomet image-analysis software.

All experiments were performed using the Pocket Jaw unit of the Gleeble 3800 complex.

Development of the austenitization model for complex microstructures of investigated steels required data on volume fractions of the structural components (ferrite, pearlite, bainite, martensite) and ferrite grain sizes (see Section 3), their experimental determination with acceptable accuracy being almost impossible. Therefore, the calculated values of noted parameters were used, obtained with the help of previously developed computer program

AusEvol Pro [20], that enables the calculation of the austenite decomposition under arbitrary cooling taking into account the effects of steel chemical composition. Performing these calculations requires data on the initial austenite grain size. Therefore, for each of the steels under consideration the austenite grain size, formed during the selected austenitization treatment (heating (5°C/s) up to 1000°C → exposure 60 s), was determined. For this purpose a series of experiments on austenite decomposition under continuous cooling with formation of special microstructures, allowing to reveale the boundaries of former austenite grains was carried out. For steels 45Х and 65Г pearlite microstructures with a ferrite grid along the boundaries of former austenite grains were used, obtained as a result of cooling from 900°C with a suitable rate. In case of steels 12Х1МФ, 13ХФА and АБ2 the samples were cooled from 900°C at the rate of 1°C/s to a temperature chosen equal to the temperature corresponding to ~ 10÷15% of austenite decomposition with formation of ferrite. After that samples were cooled at rate of 200°C/s. Such cooling regime ensured decoration of the boundaries of austenite grains with a ferrite grid, which clearly manifested itself against the background of martensitic structures during etching. In case of steels 18ХГНМФР, 14ХГ2САФД and S690 bainitic microstructures (mainly of lath morphology), obtained by cooling from 900°C with a specific rate for each steel, were used to identify the discussed boundaries.

Preparation of appropriate samples for metallographic studies and measurements of the austenite grain size were performed using the above mentioned equipment.

Results used in model calibration. Initial microstructures of the steels used for studying the austenitization include ferritic-pearlitic (PF (polygonal ferrite) + PE), ferritic-bainitic (PF + B), pearlitic-martensitic (PE + M), bainitic-martensitic (B + M) and other more complex ones. Examples of corresponding microstructures for a number of steels obtained at different rates of austenite cooling are shown in Fig. 1.

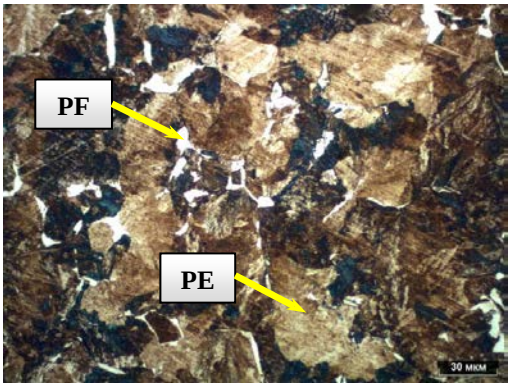

a) 1°C/s

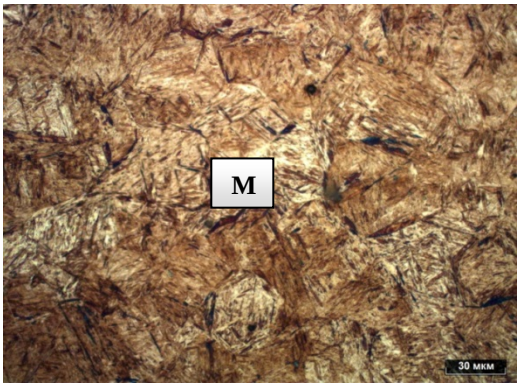

b) 100°C/s

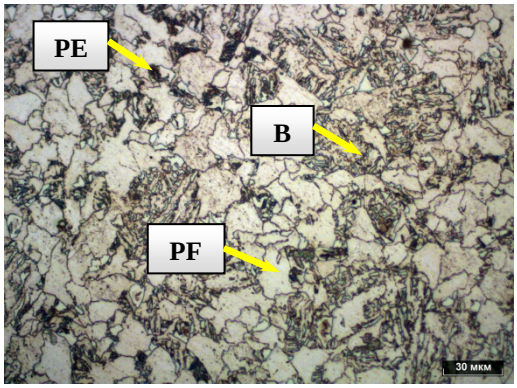

c) 1°C/s

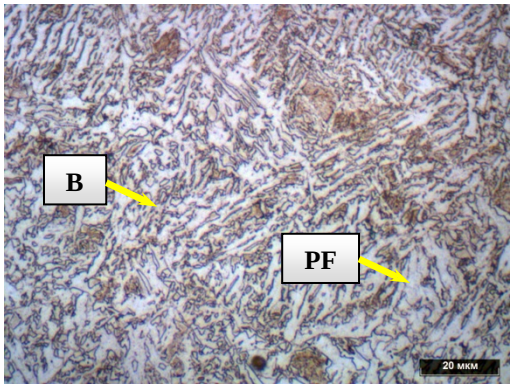

d) 10°C/s

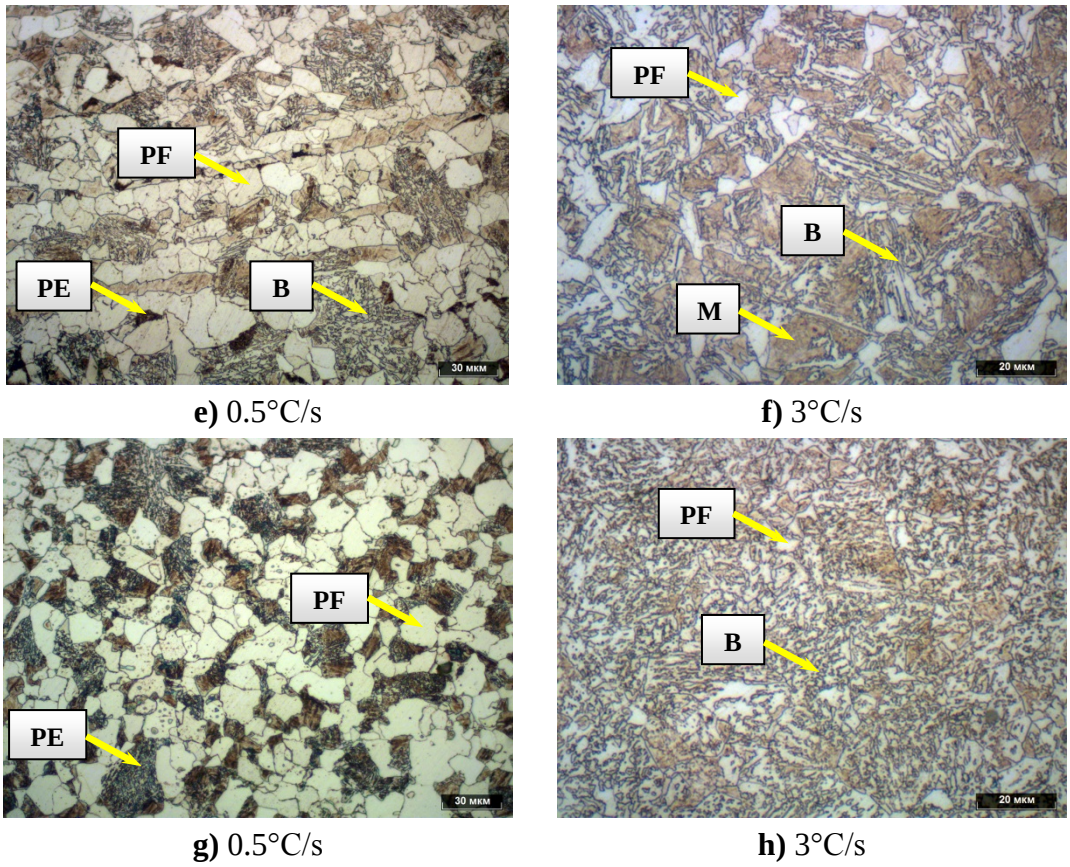

e) 0.5°C/s **f)** 3°C/s

g) 0.5°C/s **h)** 3°C/s

Fig. 1. Examples of microstructures, used for studying the austenitization, obtained under continuous cooling of austenite with different cooling rates. **45X:** PF + PE (a), M (b); **АБ2:** PF + PE + B (c), PF + B (d); **14ХГ2САФД:** PF + PE + B (e), PF + B + M (f); **S690:** PF + PE (g), PF + B (h)

The calculated volume fractions of the structural components and ferrite grain sizes (in initial microstructures) used in model calibration (see Section 3) are presented in Table 2. In general, the predicted types of microstructures are in good agreement with experimentally observed ones. At the same time, for some of steels and cooling rates, there are insignificant discrepancies between calculation results and experiment. The austenite grain sizes, for which calculations were carried out, as well as heat treatment mode used to obtain corresponding special microstructures, are given in Table. 3. Examples of such microstructures for steels 45X and 14ХГ2САФД and results of their analysis with the help of the Thixomet software are presented in Fig. 2.

Table 2. Calculated volume fractions of the structural components (PF, PE, B, M) and ferrite grain sizes (D_α). Actual and predicted types of the microstructures and corresponding austenite cooling rates (CR) are listed. The predicted types of microstructures that differ from those observed experimentally are highlighted in gray

Steel	CR, °C/s	Initial microstructure		Calculated volume fraction, %				D_α, μm
		Actual	Predicted	PF	PE	B	M	
45X	1	PF + PE	PF + PE	30.5	69.5	0.0	0.0	11.1
	100	M	PE + M	0.0	2.2	0.0	97.8	–
65Г	3	PF + PE	PE + M	0.0	99.9	0.0	0.1	–
	30	PE + M	PE + M	0.0	5.8	0.0	94.2	–

12Х1МФ	1	PF + PE + B	PF + PE	86.5	13.5	0.0	0.0	11.9
	30	B + M	B + M	0.0	0.0	83.1	16.9	–
13ХФА	1	PF + PE	PF + PE	87.0	13.0	0.0	0.0	12.9
	30	PF + B	PF + B	75.5	0.0	24.4	0.0	7.2
АБ2	1	PF + PE + B	PF + PE	90.8	9.2	0.0	0.0	12.6
	10	PF + B	PF + B	50.7	0.0	49.3	0.0	6.7
18ХГНМФР	1	B + M	B + M	0.0	0.0	32.9	67.1	–
14ХГ2САФД	0.5	PF + PE + B	PF + PE	77.9	22.1	0.0	0.0	14.7
	3	PF + B + M	PF + PE + B	71.7	22.5	5.8	0.0	6.2
S690	0.5	PF + PE	PF + PE	87.4	12.6	0.0	0.0	9.1
	3	PF + B	PF + B	21.8	0.0	78.2	0.0	2.6

Table 3. Austenite grain sizes (D_γ) obtained using special microstructures and corresponding cooling regimes (RT – room temperature)

Steel	Cooling regime	D_γ, μm
45Х	900°C → RT (1°C/s)	48
65Г	900°C → RT (3°C/s)	42
12Х1МФ	900°C → 757°C (1°C/s) → RT (200°C/s)	33
13ХФА	900°C → 798°C (1°C/s) → RT (200°C/s)	30
АБ2	900°C → 698°C (1°C/s) → RT (200°C/s)	34
18ХГНМФР	900°C → RT (0.2°C/s)	28
14ХГ2САФД	900°C → RT (10°C/s)	46
S690	900°C → RT (10°C/s)	12

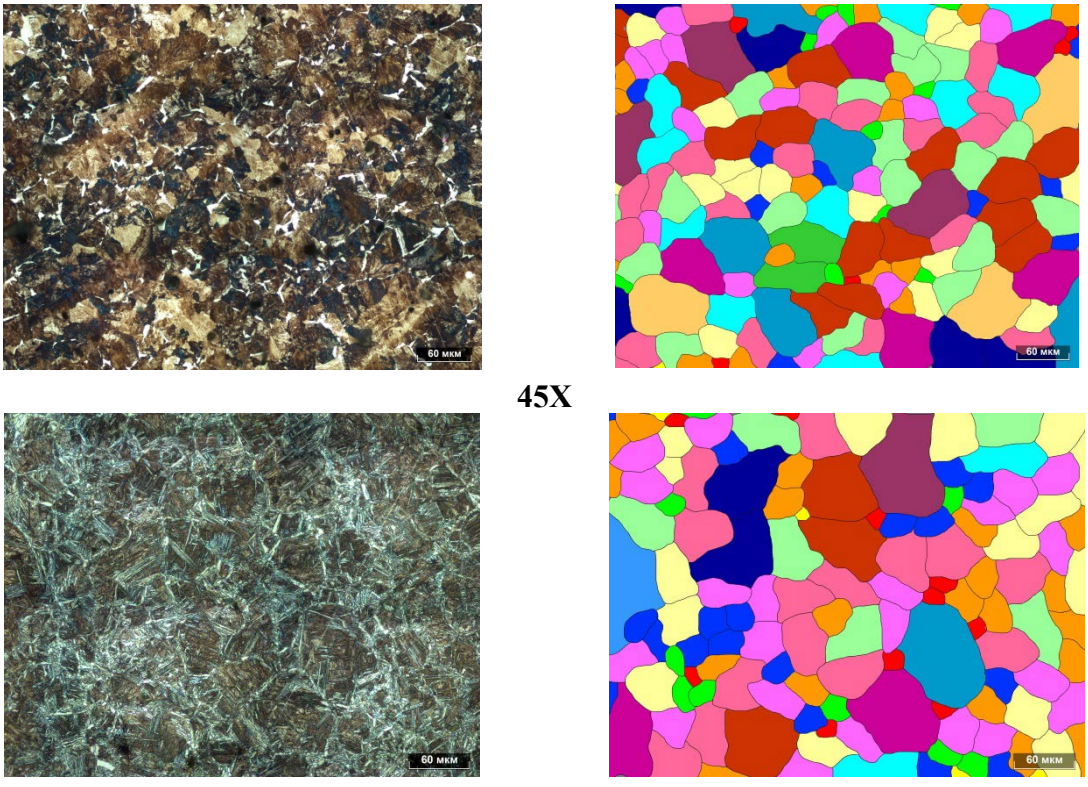

Fig. 2. Examples of the microstructures used to determine the austenite grain size (left) and images of restored austenite grain structure obtained with the help of Thixomet (right)

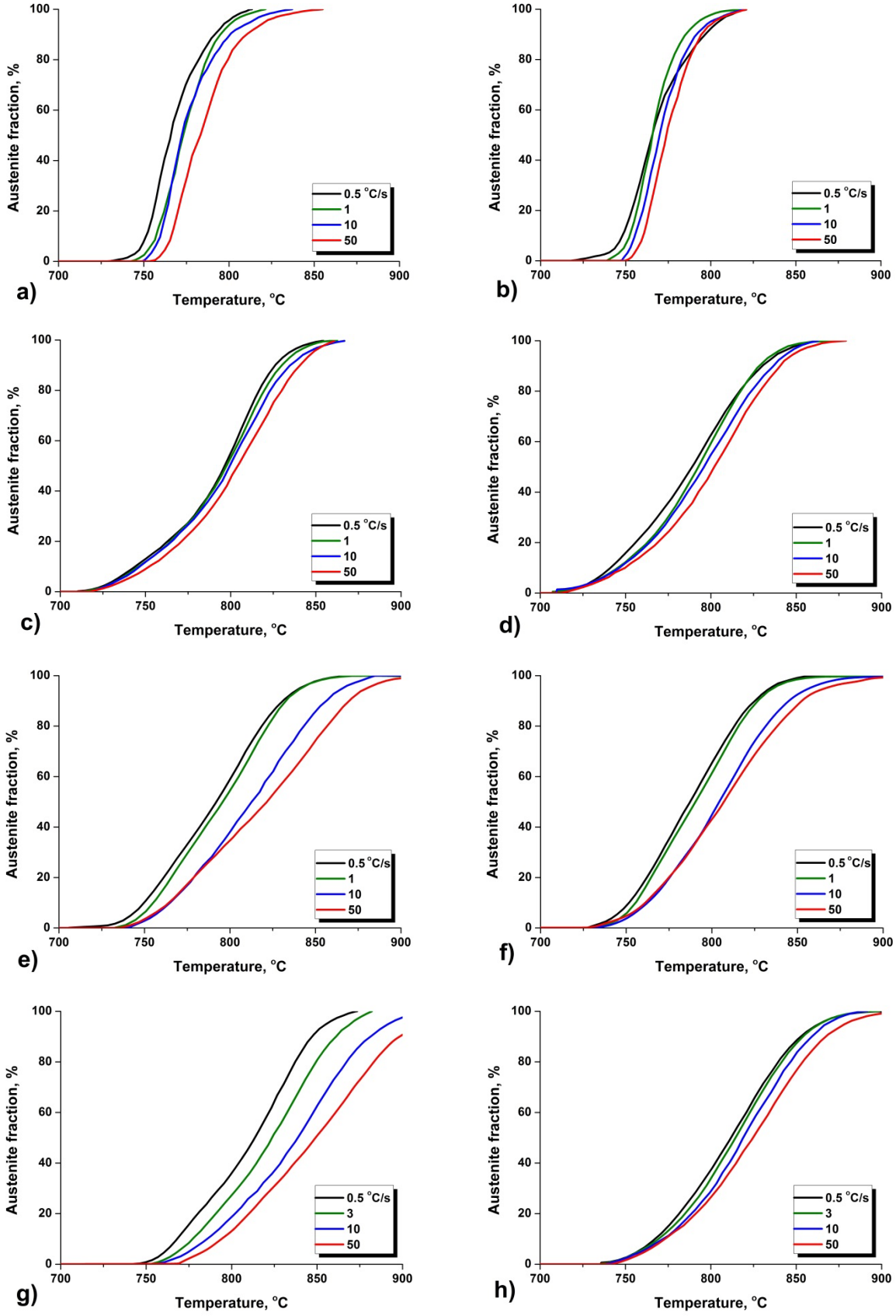

Fig. 3. Experimental austenitization curves for different heating rates of a number of investigated steels with different initial microstructures. **45Х:** PF + PE (a), M (b); **АБ2:** PF + PE + B (c), PF + B (d); **14ХГ2САФД:** PF + PE + B (e), PF + B + M (f); **S690:** PF + PE (g), PF + B (h)

Examples of the obtained austenitization curves are shown in Fig. 3. Based on the results obtained, the following conclusions can be drawn:

1. For all steels and their initial microstructures the austenitization curves are significantly shifted to higher temperatures compared to curves of the para-equilibrium austenite fraction change with temperature calculated using equation (11). In other words, the austenitization takes place under conditions of a substantial overheating.

2. Beginning of the transformation takes place in a rather narrow temperature range.

3. There is a weak dependence of the austenitization kinetics on the heating rate. This is expressed in the fact that corresponding sets of curves form a dense "bundles" (Fig. 3b, c, d, h). More pronounced dependence on the heating rate occurs for microstructures with a significant volume fraction of ferrite (Fig. 3a, e, g). This effect indicates that there are physical mechanisms that lead (other things being equal) to acceleration of the austenitization kinetics with increasing heating rate.

3. Description of the model, its calibration and obtained results

Austenite grains nucleation. According to experimental observations it is supposed that nucleation of the austenite grains occurs on the cementite particles/plates. Three modes of nucleation are considered:

- at the edges of cementite plates on the surface of pearlite colonies (1 mode);
- on particles of tertiary cementite located at the ferrite grain boundaries (mode 2);
- on cementite particles inside the volumes of bainite and martensite formed during decomposition of austenite and subsequent heating of obtained structures (3 mode).

Austenite formation becomes thermodynamically favorable when the following condition is satisfied: $\Delta G_{\alpha\to\gamma}\left(T,Y_{AE}\right)<0$, where $\Delta G_{\alpha\to\gamma}\left(T,Y_{AE}\right)$ is the thermodynamic driving force of the transformation under consideration, which is calculated as:

$$\Delta G_{\alpha\to\gamma}\left(T,Y_{AE}\right)=\frac{G_{\gamma}\left(T,Y_{AE}^{*}\right)-\left(\sum_{X} y_X \mu_X^{\alpha}\left(T,Y_{AE}\right)+y_C\mu_C^{\alpha}\left(T,Y_{AE}\right)\right)}{\Omega_{\gamma}^{m}}, \quad (1)$$

where $G_{\gamma}\left(T,Y_{AE}^{*}\right)$ is Gibbs molar energy of austenite; $Y_{AE}=\left\{y_C,y_{Mn},y_{Si},y_{Cr},y_{Ni},y_{Cu},y_{Mo}\right\}$ is the set of average concentrations (site fractions) of the alloying elements in solid solution; y_C is the portion of interstitial sublattice sites occupied by carbon atoms; y_X is the portion of substitution sublattice sites occupied by the atoms of element *X* (*X = Mn, Si, Cr, Ni, Cu, Mo*); $Y_{AE}^{*}=\left\{y_C^{*},y_{Mn},y_{Si},y_{Cr},y_{Ni},y_{Cu},y_{Mo}\right\}$, where $y_C^{*}=y_{C\gamma/\theta}^{eq}$ is equilibrium carbon concentration in austenite at the austenite/cementite interface (hereinafter the para-equilibrium carbon concentrations are used); $\mu_X^{\alpha}\left(T,Y_{AE}\right)$, $\mu_C^{\alpha}\left(T,Y_{AE}\right)$ are, respectively, the chemical potentials of element *X* and carbon in ferrite; Ω_{γ}^{m} is the austenite molar volume.

For all the modes it is assumed that nucleation time is small, and when the thermodynamic condition is fulfilled a fixed number of the austenite grains nuclei are formed. The nuclei volume density for the first mode is calculated as:

$$N_{\gamma 1}=\alpha_{N1}^{PE}\ f_{PE}^{0\ 2/3}, \quad (2)$$

where f_{PE}^{0} is volume fraction of perlite in the initial microstructure; α_{N1}^{PE} is an empirical parameter.

Austenite nuclei volume density for the second mode is calculated as:

$$N_{\gamma 2} = \alpha_{N2}^{\theta} \frac{w_C^{\theta}}{D_{\alpha}} f_{PF}^{0}, \tag{3}$$

where w_C^{θ} is carbon content in austenite at the moment of completion of its transformation under cooling (mass.%), which determines a volume fraction of tertiary cementite in initial (before the heating starts) steel microstructure; f_{PF}^{0} is volume fraction of ferrite in these microstructures; D_{α} is ferrite grain size; α_{N2}^{PE} is an empirical parameter.

For the third mode the nuclei volume density is calculated as:

$$N_{\gamma 3} = w_C^{B+M} \left(\alpha_{N3}^{B} f_B^0 + \alpha_{N3}^{M} f_M^0 \right), \tag{4}$$

where w_C^{B+M} is content of carbon "trapped" in the volume of bainitic-martensitic part of microstructure during decomposition of austenite; f_B^0, f_M^0 are, accordingly, initial volume fractions of bainite and martensite; $\alpha_{N3}^{B}, \alpha_{N3}^{M}$ are empirical parameters.

For the volume density of all austenite grains nuclei we have:

$$N_{\gamma} = \sum_{i=1}^{3} N_{\gamma i}. \tag{5}$$

Austenite grains growth. Growth rate of the austenite grains is determined by the type of the consumed component of initial microstructure. In case of its growth into pearlite this rate is calculated as [15]:

$$V_{\gamma}^{PE}\left(T, Y_{AE}\right) = \alpha_{HR}^{PE}\left(R_H\right) \frac{\bar{D}_C\left(T, Y_{AE}\right)}{\lambda} \frac{\left(C_{\gamma/\theta}^{\gamma} - C_{\gamma/\alpha}^{\gamma}\right)}{\left(C_{\theta} - \bar{C}_{PE}\right)}, \tag{6}$$

where $\bar{D}_C\left(T, Y_{AE}\right)$ is coefficient of carbon volume diffusion in austenite [21] averaged over its concentration profile in this phase (averaging is carried out in the interval $\left[C_{\gamma/\theta}^{\gamma}, C_{\gamma/\alpha}^{\gamma}\right]$); λ is the interlamellar spacing in pearlite; $C_{\gamma/\theta}^{\gamma}, C_{\gamma/\alpha}^{\gamma}$ are, respectively, the equilibrium concentrations of carbon in austenite at its interface with cementite and ferrite; C_{θ} is carbon concentration in cementite; $\bar{C}_{PE}$ is an average carbon concentration in pearlite; $\alpha_{HR}^{PE}\left(R_H\right) = 1 + \beta_{HR}^{PE} R_H$ is a factor that takes into account austenite growth rate dependence on the heating rate R_H (°C/s); β_{HR}^{PE} is an empirical parameter. Use of austenite growth rate in pearlite depending on the heating rate based on experimental data shows that this process accelerates with increasing heating rate [4,5,11].

In case of the austenite grains growth into ferrite, bainite and martensite it is assumed that rate of the γ/α–interface movement is governed by the diffusion controlled lattice reconstruction and is calculated as:

$$\begin{gathered} V_{\gamma}^{k}\left(T, Y_{AE}\right) = -\alpha_{HR}^{k}\left(R_H\right) M_{\gamma/\alpha}^{k}\left(T\right) \Delta G_{\alpha\to\gamma}\left(T, Y_{AE}^{**}\right), \\ M_{\gamma/\alpha}^{k}\left(T\right) = M_{\gamma/\alpha 0}^{k}\, exp\left(-\frac{Q}{RT}\right), \end{gathered} \tag{7}$$

where $\Delta G_{\alpha\to\gamma}\left(T, Y_{AE}^{**}\right)$ is the thermodynamic driving force calculated for carbon concentration in austenite equal to its equilibrium value at the interface with ferrite $y_C^{**} = y_{C\gamma/\alpha}^{\gamma}$; $M_{\gamma/\alpha}^{k}\left(T\right)$ is the interface mobility; Q is the process activation energy depending on chemical composition and considered as empirical parameter of the model; $\alpha_{HR}^{k}\left(R_H\right) = 1 + \beta_{HR}^{k} R_H$ is factor that

takes into account the dependence of austenite growth rate on the heating rate (similar in meaning to the factor $\alpha_{HR}^{PE}(R_H)$); $M_{\gamma/\alpha 0}^{k}, \beta_{HR}^{k}$ are empirical parameters; k = PF, B + M.

Because of the complexity of detailed description of the austenite grains growth with account of difference in rates of corresponding boundary movement into volumes of different structural components, it was assumed that their growth is isotropic. To calculate an effective growth rate of spherical grains with account of volume fractions of the components the following expression is used:

$$V_\gamma = \sum_k V_k\left(T, Y_{AE}\right) f_k, \tag{8}$$

where $f_k = f_k(t)$ is a current volume fraction of the $k-$th component of microstructure; k = PF, PE, M. Accordingly, the radius of austenite grains at time t is calculated as:

$$R_\gamma(t) = \int_0^t V_\gamma(\tau)\, d\tau. \tag{9}$$

With account of contribution of a "hard" collisions of growing austenite grains to the increments of its volume fraction due to their growth into pearlite, ferrite and bainite/martensite one may write down:

$$df_{au}^{k}(t) = 4\pi\left(1-\sum_k f_{au}^{k}(t)\right) N_{\gamma k} R_\gamma^2(t) V_k(t)\, dt, \tag{10}$$

where $f_{au}^{k}(t)$ is the volume fraction of austenite formed at time t due to its growth into $k-$th component of the initial microstructure (k = PF, PE, M); $\sum_k f_{au}^{k}(t)$ is a total volume fraction of austenite.

When calculating increments of the austenite volume fraction, it is taken into account that at any temperature this fraction cannot exceed the equilibrium value:

$$f_\gamma^{eq} = \frac{w_C - w_{C_{\gamma/\alpha}}^{\alpha}}{w_{C_{\gamma/\alpha}}^{\gamma} - w_{C_{\gamma/\alpha}}^{\alpha}}, \tag{11}$$

where w_C is carbon content in steel (mass.%); $w_{C_{\gamma/\alpha}}^{\gamma}, w_{C_{\gamma/\alpha}}^{\alpha}$ are, accordingly, equilibrium carbon contents in austenite and ferrite at the γ/α–interface (mass.%).

The average final austenite grain size (diameter) is calculated as:

$$D_\gamma = \left(\frac{2}{3N_\gamma}\right)^{1/3}. \tag{12}$$

Model calibration and obtained results. Calibration of the model was made on the basis of obtained experimental data using calculated volume fractions of the structural parameters obtained with the help of computer program AusEvol Pro. Carbon contents in austenite at the moment of completion of its transformation during cooling, and the carbon content “captured” inside the volume of bainitic-martensitic part of the formed microstructures were also calculated.

The set of optimal values of the model empirical parameters was determined as a result of its calibration performed using the developed computer program. The values of these parameters are given in Table 4.

Table 4. Values of the model empirical parameters

Nucleation parameters	$\alpha_{N1}^{PE} = 5\times10^{13}\ \mathrm{m}^{-3}$ $\alpha_{N2}^{\theta} = 5\times10^{11}\ \mathrm{m}^{-2}$ $\alpha_{N3}^{B} = 1.0\times10^{15}\ \mathrm{m}^{-3}$ $\alpha_{N3}^{M} = 1.7\times10^{16}\ \mathrm{m}^{-3}$
Growth parameters	$Q = 124400 - 160 w_C^{int}(T)^{-0.9} + 3000 w_{Mn} + 15000 w_{Cr}^{0.5}$ (J/mol), $w_C^{int}(T) = 0.5\left(w_{C_{\gamma/\alpha}}^{\alpha}(T) + w_{C_{\gamma/\alpha}}^{\gamma}(T)\right)$ – effective value of carbon interfacial concentration (mass.%) $M_{\gamma/\alpha 0}^{PF} = 5.20\times10^{-9}\ \mathrm{m^3N^{-1}s^{-1}}$ $M_{\gamma/\alpha 0}^{B+M} = 2.25\times10^{-8}\ \mathrm{m^3N^{-1}s^{-1}}$
Parameters of the heating rate dependences	$\alpha_{HR}^{PE}(R_H) = 1 + 1.4R_H$ $\alpha_{HR}^{PF}(R_H) = 1 + 3.6R_H$ $\alpha_{HR}^{B+M}(R_H) = 1 + 3.5R_H$

The calculated austenitization curves for a number of studied steels with different initial microstructures together with experimental data are presented in Fig. 4. As one can see, the developed model accurately reproduces kinetics of the process in a wide range of heating rates. Average absolute value of relative error in calculating the austenitization curves is equal to 9.4%. Predicted values of austenite grain size are also in good agreement with experimental data (Fig. 5). Note, that the average absolute value of relative error in calculating the grain size does not exceed 17.5%, which is comparable with the corresponding error of its measurements.

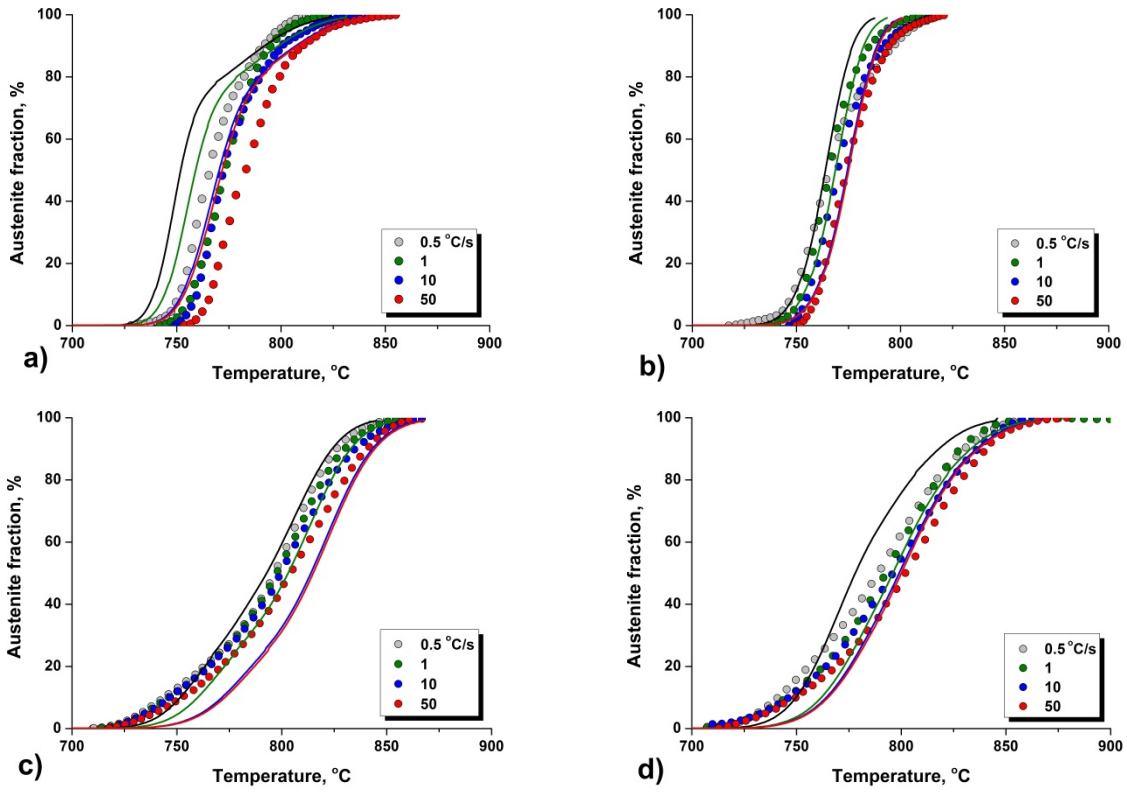

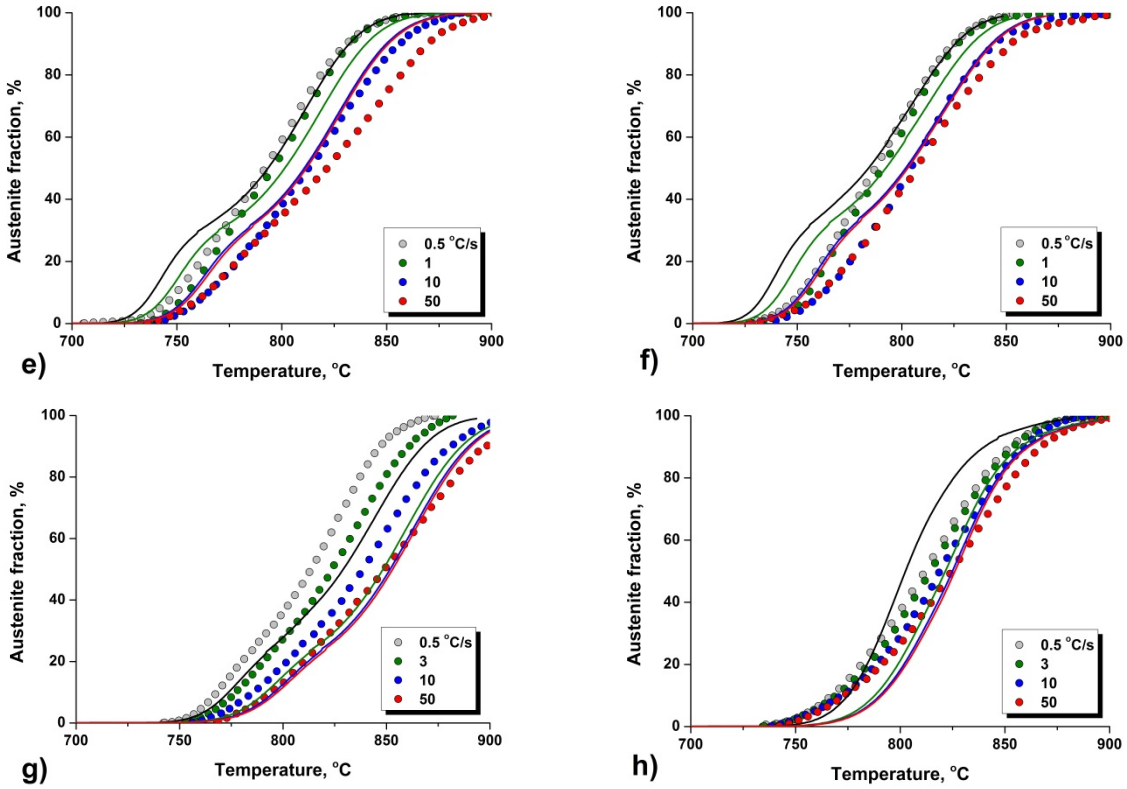

Fig. 4. Calculated austenitization curves for different heating rates of a number of investigated steels with different predicted microstructures in comparison with experimental data (symbols). **45Х:** PF + PE (a), M (b); **АБ2:** PF + PE + B (c), PF + B (d); **14ХГ2САФД:** PF + PE + B (e), PF + B + M (f); **S690:** PF + PE (g), PF + B (h)

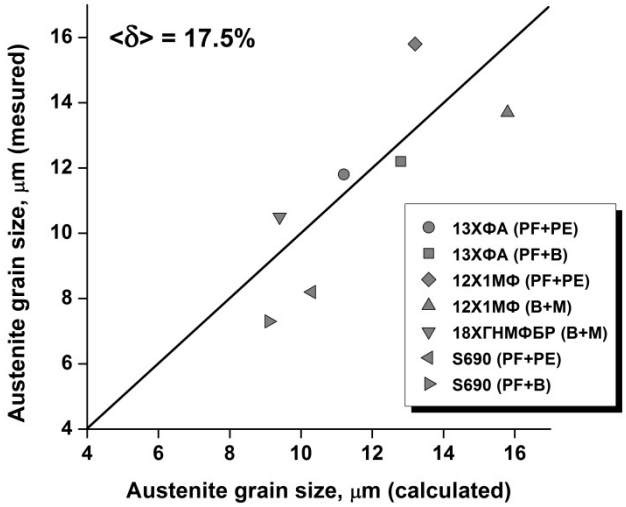

Fig. 5. Comparison of the calculated and measured austenite grain sizes for various steels. <δ> is the average absolute value of the relative error of calculations

4. Conclusions

An experimental investigation of the kinetics of austenitization under continuous heating of various complex microstructures of 8 industrial steel grades with wide range of chemical compositions (C(0.08÷0.66), Mn(0.37÷1.55), Si(0.20÷0.56), Cr(0.10÷1.08), Ni(0.06÷1.94), Mo(0.01÷0.52), Nb(0.003÷0.041), V(0.002÷0.15), Ti(0.002÷0.063) (mass.%)) was carried out. A quantitative mathematical model has been developed to describe the kinetics of

austenitization and to predict the final austenite grain size. The set of empirical model parameters was determined on the basis of the obtained data on kinetics of the process. Additionally, when calibrating the model, a calculated data set on parameters of initial microstructures of steels obtained using a previously developed computer model of austenite decomposition was used.

The obtained results show that the developed model correctly reproduces the kinetics of austenitization in a wide range of heating rates. The results of predicting the final austenite grain size also agree well with experimental data.

Acknowledgments. *This work was supported by grant from Russian Science Foundation (project No. 17-19-01178).*

References

[1] Speich GR, Szirmae A. Formation of austenite from ferrite and ferrite-carbide aggregation. *Transactions Metallurgical Society AIME*. 1969;245: 1063-1074.
[2] Garcia CI, De Ardo AJ. Formation of austenite in 1.5 pct. Mn steels. *Metallurgical Transactions: A*. 1981;12(3): 521-530.
[3] Speich GR, Demarest VA, Miller RL. Formation of austenite during intercritical annealing of dual-phase steels. *Metallurgical Transactions: A*. 1981;12(8): 1419-1428.
[4] Caballero FG, Capdevila C, Garcia de Andres C. Influence of pearlite morphology and heating rate on the kinetics of continuously heated austenite formation in a eutectoid steel. *Metallurgical Transactions: A*. 2001;32(6): 1283-1291.
[5] Caballero FG, Capdevila C, Garcia de Andres C. Modelling of kinetics of austenite formation in steels with different initial microstructures. *Iron and Steel Institute of Japan International*. 2001;41(10): 1093-1102.
[6] Huang J, Poole WJ, Militzer M. Austenite formation during intercritical annealing, *Metallurgical Transactions: A*. 2004;35(11): 3363-3375.
[7] Schmidt E, Wang Y, Sridhar S. A study of nonisothermal austenite formation and decomposition in Fe-C-Mn alloys. *Metallurgical Transactions: A*. 2005;37(6): 1799-1810.
[8] Savran VI, Van Leeuven Y, Hanlon DN, Kwakernaak C, Sloof WG, Sietsma J. Microstructural features of austenite formation in C35 and C45 alloys. *Metallurgical Transactions: A*. 2007;38(5): 946-955.
[9] Martin D, Cock T, Garcia-Junceda A, Caballero FG, Capdevila C, Garcia de Andres C. Effect of heating rate on reaustenitization of low carbon niobium microalloyed steel. *Journal of Materials Science and Technology*. 2008;24: 266-272.
[10] Asadi Asadabad M, Goodarzi M, Kheirandish S. Kinetics of austenite formation in dual phase steels. *Iron and Steel Institute of Japan International*. 2008;48(9): 1251-1255.
[11] Caballero FG, Capdevila C, Garcia de Andres C. An attempt to establish the variables that most directly influence the austenite formation process in steels. *Iron and Steel Institute of Japan International*. 2003;43(5): 726-735.
[12] Savran VI, Offerman SE, Sietsma J. Austenite nucleation and growth observed on the level of individual grains by three-dimensional X-ray diffraction microscopy. *Metallurgical Transactions: A*. 2010;41(3): 583-591.
[13] Mohanty RR, Girina OA, Fonstein NM. Effect of heating rate on the austenite formation in low-carbon high-strength steels annealed in the intercritical region. *Metallurgical Transactions: A*. 2011;42: 3680-3690.
[14] Azizi-Alizamini H, Militzer M, Poole WJ. Austenite formation in plain low-carbon steels. *Metallurgical Transactions: A*. 2011;42(6): 1544-1557.

[15] Golikov PA, Zolotorevsky NYu, Vasilyev AA. Modeling kinetics of $\alpha \rightarrow \gamma$ transformation in steels with ferretic-pearlitic microstructure. *Scientific and Technical Statements SPbSPU*. 2011;129(3): 110-117.
[16] Senuma T. Present status and future prospects of simulation models for predicting the microstructure of cold-rolled steel sheets. *Iron and Steel Institute of Japan International*. 2012;52(4): 679-687.
[17] Kulakov M, Poole WJ, Militzer M. The effect of the initial microstructure on recrystallization and austenite formation in a DP600 steel. *Metallurgical Transactions: A*. 2013;44(8): 3564-3576.
[18] Kulakov M, Poole WJ, Militzer M. A microstructure evolution model for intercritical annealing of a low-carbon dual-phase steel. *Iron and Steel Institute of Japan International*. 2014;54(11): 2627-2636.
[19] Zhu B, Militzer M. Phase-field modeling for intercritical annealing of a dual-phase steel. *Metallurgical Transactions: A*. 2015;46(3): 1073-1084.
[20] Sokolov DF, Sokolov SF, Vasilyev AA. *AusEvol Pro: the program for modeling of steel microstructure and mechanical properties (Program Instructions, in English).* 2014618758 (Certificate of state registration of the computer program), 2014.
[21] Vasilyev A. Carbon diffusion coefficient in complexly alloyed austenite. *Proceedings of the conference "Materials Science and Technology 2007"*. 2007: 537-551.